

# Sedimentary and hydrological studies of the Holocene palaeofloods in the Shanxi-Shaanxi Gorge of the middle Yellow River, China

Xiaogang Li · Chun Chang Huang · Jiangli Pang · Xiaochun Zha · Yugai Ma

Received: 11 October 2013 / Accepted: 29 July 2014 / Published online: 23 August 2014  
© Springer-Verlag Berlin Heidelberg 2014

**Abstract** Holocene slackwater deposits along the river channels were used to study the magnitude and frequency of the palaeofloods that occurred prior to gauged and historical data sets all over the world. Palaeohydrological investigations along the Shanxi-Shaanxi Gorge of the middle Yellow River, China, identified palaeoflood slackwater deposits (SWDs) at several sites along the cliffs bordering the river channel. The SWDs are intercalated within Holocene eolian loess-soil profiles and clastic slope deposits. The palaeoflood SWDs were differentiated from eolian loess and soil by the sedimentary criteria and analytical results including magnetic susceptibility and particle-size distribution, similar to the flood SWDs in 2012, which indicated that these well-sorted palaeoflood SWD beds were deposited from the suspended sediment load in floodwaters. They have recorded the extraordinary palaeoflood events which occurred between 3200 and 3000 a BP as dated by the optically stimulated luminescence method in combination with pedostratigraphic correlations with the previously studied Holocene pedo-stratigraphy in the Yellow River drainage basin. Manning slope-area calculations estimate the peak discharged for these palaeoflood events to range from 43,290 to 49,830 m<sup>3</sup>/s. The drainage area of the study site is 489,900 km<sup>2</sup>. It is 2.0–2.5 times the largest gauged flood (21,000 m<sup>3</sup>/s) that has ever occurred since 1934. These events also occurred on Yellow River

tributaries, including the Weihe, Jinghe and Qishuihe Rivers. These flood events are therefore considered to be a regional expression of known climatic events in the northern hemisphere and demonstrate Holocene climatic instability. This study provides important data in understanding the interactions between regional hydro-climatic systems and global change in semiarid and subhumid regions.

**Keywords** Palaeoflood · Slackwater deposit · Holocene · Yellow river · China

## Introduction

Global Flood damages are increasing at a spectacular rate (Baker 2006). Extreme flooding and drought are often connected with anomalous atmospheric circulation patterns and hydrological change in response to global climate change (Huang et al. 2012a, 2013). Palaeoflood hydrological investigations enable the linkages between extreme events in fluvial systems and global change to be studied over long timescales (Knox 2000; Huang et al. 2010, 2011, 2012b). As a kind of regional fluvial process, overbank flooding often leaves sedimentary records over the inundated areas in their paths (Baker and Kochel 1988; Benito et al. 2003a, b; Huang et al. 2010). Bedded sequences of flood slackwater deposits (SWDs) along a river valley record individual floods. Palaeoflood SWDs are fine-grained sediments conveyed in suspension during highly energetic flood flows and deposited in areas of flow separation that result in long-term preservation after the flood recession (Baker and Kochel 1988; Baker 2006). They are studied with the multidisciplinary methods of fluvial geomorphology, Quaternary sedimentology and geochronology for identification of palaeoflood stages,

X. Li · C. C. Huang (✉) · J. Pang · X. Zha · Y. Ma  
Department of Geography, Shaanxi Normal University,  
Xi'an 710062, Shaanxi, People's Republic of China  
e-mail: cchuang@snnu.edu.cn

X. Li  
Department of Urban–Rural Development and Management  
Engineering Science, Shangluo University, Shangluo 726000,  
Shaanxi, People's Republic of China

and further for estimation of palaeoflood discharges using hydraulic calculation models (Baker 1987, 2006, 2008). Thus, palaeoflood study will also play an important role in mitigating flood risks and in improving flood design in hydraulic engineering (Benito et al. 2004; Benito and Thorndyraft 2005).

The Yellow River is famous for the birthplace of the four ancient civilizations as well as the Indian River, the Ganges, the Nile and the Mesopotamia. Extremely high sediment discharge ( $1.6 \times 10^9$  tonnes/a, the highest sediment discharge in the world) and flood disasters are of concern to geographers and hydrologists in the Yellow River. The 1982 flood peak discharges was gauged at 15,300 m<sup>3</sup>/s at the Huayuankou gauge station in the middle reaches of the Yellow River. That flood produced serious threats for downstream villages of 1,303, agricultural lands of over 144,960 hm<sup>2</sup> and more than 932,700 population (Yi and Shi 1997). Affected by the reduction in annual precipitation and runoff volume since the early 1980s, water resources were growing shortage in the middle Yellow River (Xu et al. 2009), and the frequency of drought and flood occurred increasing (Zhang et al. 1999; Peng et al. 2011). These phenomena indicate intensified variability and instability of the hydro-climatic system in semiarid and subhumid regions and imply that the region might have been influenced by global change. The development of water resources and water energy, the flood disaster governance, and regulation of flood hazards for the middle Yellow River should incorporate consideration of long-term flood hydrological data, i.e., palaeoflood data.

Previous investigations of middle Yellow River palaeofloods were focused on the reach from Sanmenxia to the Xiaolangdi Valley. (Yang et al. 2000). During the last 10 years, our investigations have already identified palaeoflood SWDs, determined the age of palaeoflood recorded by SWDs by using optically stimulated luminescence (OSL) dating and pedostratigraphic correlations and reconstructed palaeoflood peak stages and discharges in the Yellow River and its tributaries such as the Sushui River, the Qishuihe River, the Jinghe River, the Weihe River and the Beiluohe River (Huang et al. 2007, 2010, 2011, 2012a, b, c; Yao et al. 2008; Li et al. 2010).

This paper presents five bedsets of newly discovered palaeoflood SWDs in the Shanxi-Shaanxi Gorges, middle reach of the Yellow River (Fig. 1). We investigated the sedimentary features, chronology, and hydrological characteristics of these extraordinary flood deposits in the Shanxi-Shaanxi Gorges. These are of great significance in the understanding of the linkages between hydrological events and global climate change, as well as designed standard of flood control in hydraulic and hydroelectric engineering in the middle Yellow River.

## Geographical setting

The Yellow River originates from the Tibetan Plateau and flows eastwards to the Bohai Sea, a marginal sea in the North Pacific Ocean (Fig. 1a). The mainstream of the Yellow River is 5,464 km in length and drains a catchment area of 795,000 km<sup>2</sup>. The river is characterized by an extremely high sediment discharge of  $1.6 \times 10^9$  tonnes/a, the highest sediment discharge in the world (Xu et al. 2009). The middle reaches of the Yellow River (i.e., from the Hekou town in Inner Mongolia province to Peach blossom valley in Henan province) is 1,206.4 km long with a drainage area of 344,000 km<sup>2</sup>, in which increased runoff accounts for 42.5 % of the Yellow River water and increased sediment discharge accounts for 92 % of the Yellow River, indicating that it is the main source of Yellow River sediment because through the Loess Plateau. The middle Yellow River is divided into three sections: Hekou town–Longmen reach, Longmen–Sanmenxia reach, and Sanmenxia–Peach blossom valley reach (Fig. 1a).

The Hekou town–Longmen reach is the focus of our investigation, also known as the Shanxi-Shaanxi Gorges, which is underlain by Triassic mudstone, shale and sandstone formations. It has a typical dendritic drainage pattern draining from north to south between the Lüliangshan and the Huanglongshan Mountains. The mainstream is 723 km long with a drainage area of 111,600 km<sup>2</sup> in the Hekou town–Longmen reach. The channel drop 607 m with 400–600 m in width and the average slope is 0.00084 in the Shanxi-Shaanxi Gorges. The mean annual precipitation varies between 300 and 600 mm regionally. The regional hydro-climatic conditions are characterized by very high seasonal variability; about 61.6 % of rainfall occurs between July and September, during which the middle Yellow River drainage basin is dominated by the southeastern maritime monsoon. Great rainstorm intensity, short duration and rain zonal distribution, often form rising up and down, peaks finer lines, short duration and large sediment sudden flood.

At the Longmen gauge station (Fig. 1b), the drainage area is 497,500 km<sup>2</sup> and the length of upstream river is 4,190 km. The mean annual discharge is 958 m<sup>3</sup>/s, and the mean annual runoff volume is  $27.58 \times 10^9$  m<sup>3</sup>. The mean annual suspended sediment concentration is 29.0 kg/m<sup>3</sup> with the maximum 1,040 kg/m<sup>3</sup> occurring in 2002, and the mean annual sediment discharge is  $0.801 \times 10^9$  t (Xu et al. 2009). The largest gauged flood since 1934 with a discharge of 21,000 m<sup>3</sup>/s was record in 1967. The most recent large floods in the Hekou town–Longmen reach occurred on July 28, 2012 with a peak discharge of 7,620 m<sup>3</sup>. The highest historical flood discharge was 31,000 m<sup>3</sup>/s between 1820 and 1850. The second highest historical flood reached a discharge of 27,000 m<sup>3</sup>/s in 1931 (Yi and Shi 1997).

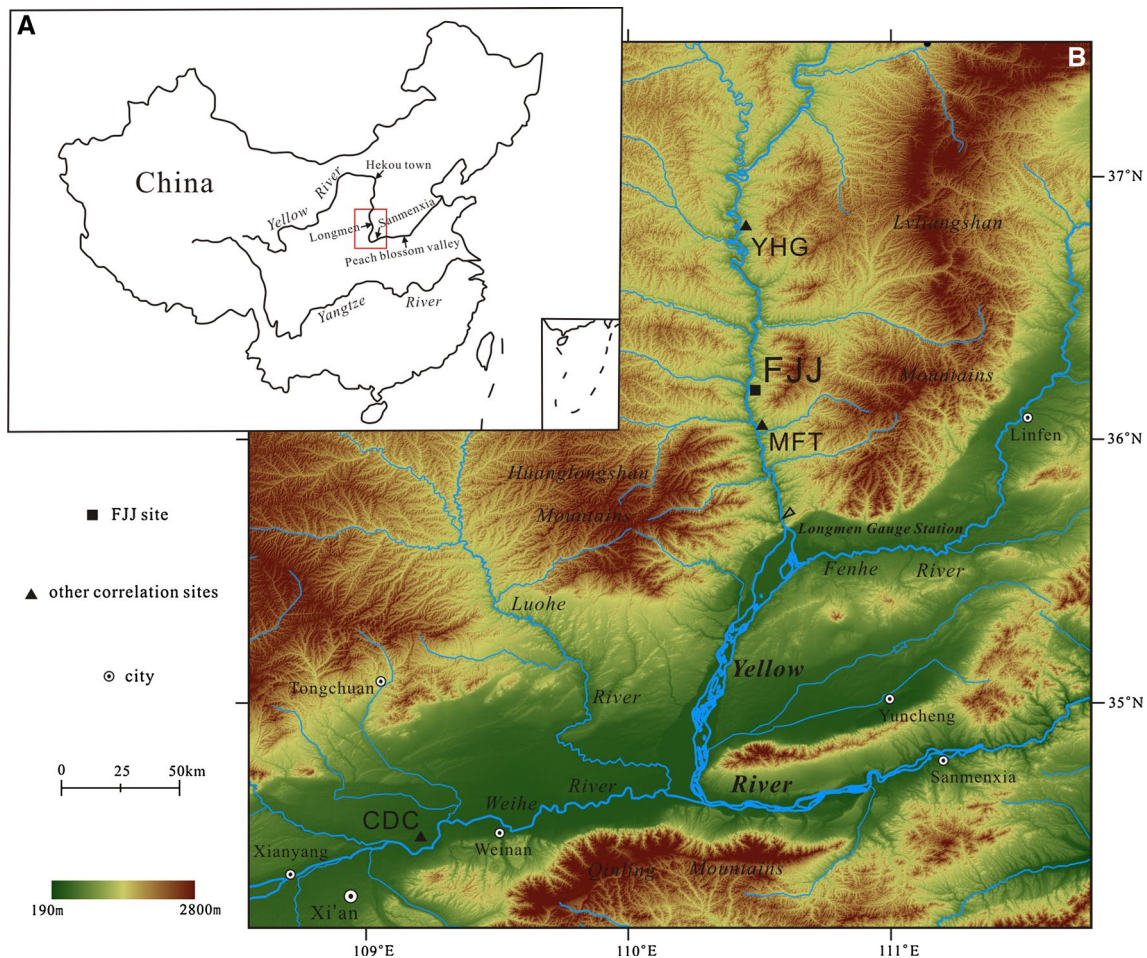


**Fig. 1** a Map showing the study reach in the Shanxi-Shaanxi Gorge in middle reach of the Yellow River in China. b The locations of the study FJJ site, and other correlation sites, where the same period palaeofloods are exposed in the Shanxi-Shaanxi Gorge of the middle Yellow River

The study site (FJJ) is in the Hekou town–Longmen reach of the Yellow River where the river has cut into the bedrock, forming a narrow and deep bedrock channel (Fig. 2a, b). The palaeoflood SWDs were identified in the Holocene loess-soil profiles in the riverbank (490 m a.s.l.), which is ca 20 m above the normal river water level, on the left side of the river (Figs. 2a, 3a). The 2012 flood slackwater deposit was found and sampled in the tributary mouths (Fig. 3c). It provides a reference for identifying palaeoflood SWDs in the Holocene loess-soil stratigraphy.

## Methods

Palaeohydrological investigations were carried out along the Shanxi-Shaanxi Gorge of the middle Yellow River between 2008 and 2012. Several palaeoflood SWD sites were found in the gorges along the river (Fig. 1b). The profile (FJJ) at the left bank of the Yellow River adjacent to the Fengjiaji village was examined and sampled for detailed

study because a set of five silt beds of fluvial deposits were found interbedded in the profile which may be able to provide information of the hydrological change on the Yellow River (Fig. 3a). Palaeoflood SWD beds recording individual flood events were identified through a variety of sedimentological criteria commonly used in the world of palaeohydrology (Baker 1987, 2006; Kale et al. 2000; Jones et al. 2001; Benito and Thorndycraft 2005; Sheffer et al. 2008; Huang et al. 2010, 2011, 2012a, b, c, 2013; Zhang et al. 2013). It was further checked by comparison with the modern flood events and their SWDs deposited on the channel sides in the same reaches. After detailed observations and pedostratigraphic subdivisions, samples for sedimentary analysis were taken every palaeoflood SWD from profile FJJ. Samples for OSL dating were taken with a steel cylinder from the profile and immediately sealed in light-proof material.

The recent flood peak stages of 2012 large flood events were marked clearly by the pale orange-colored SWDs of silt on the channel sides (Fig. 3c). Samples at the end-point

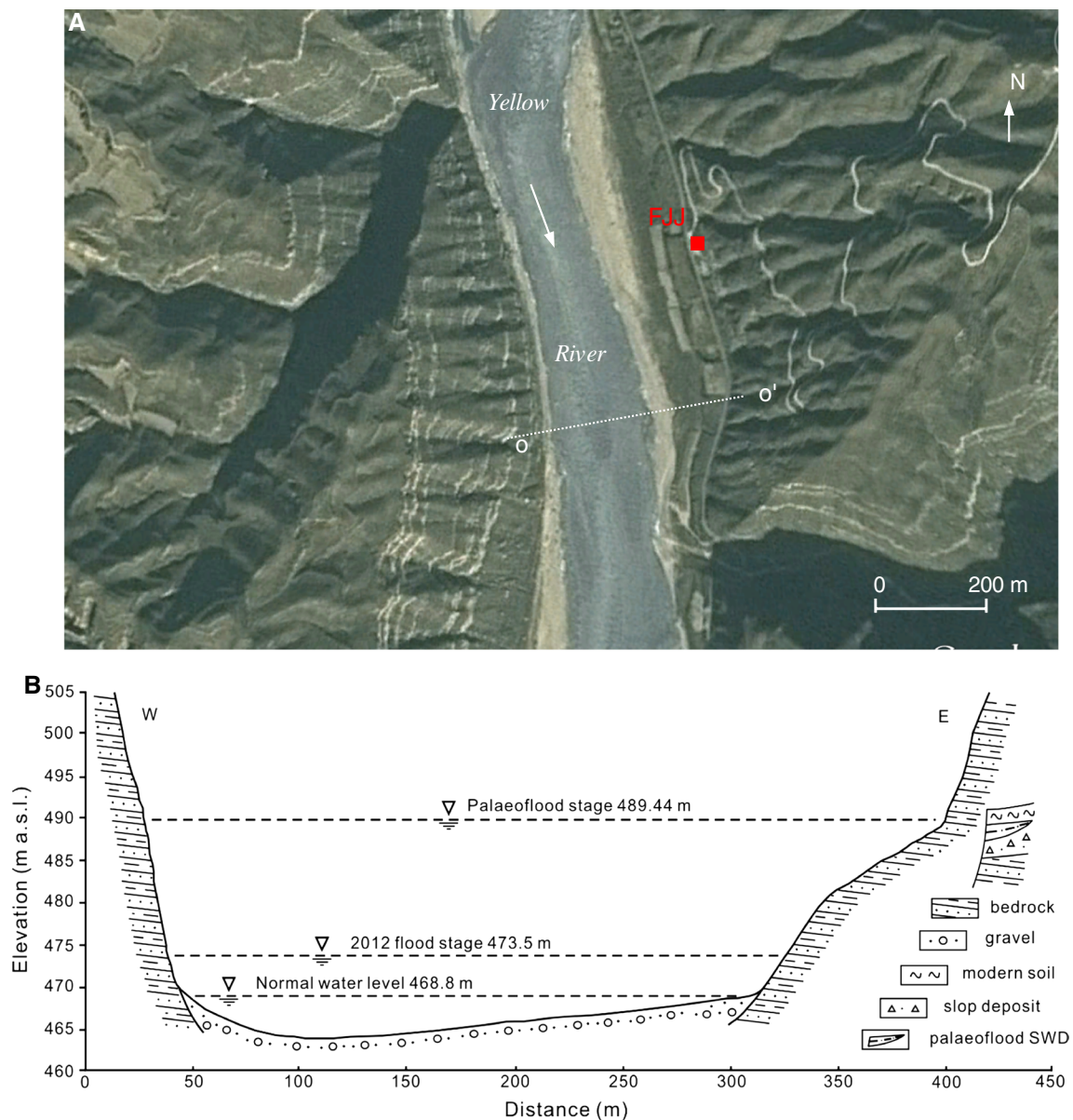


**Fig. 2** **a** The location of the Holocene sediment profile of FJJ in the Yellow River riverbank. **b** Channel section (O–O') and the lithology of the Yellow River at the Fengjiaji site (FJJ)

close to the flood stage were collected for comparison with the palaeoflood SWD in the same reaches on the Yellow River.

Magnetic susceptibility was measured on a mass of 10 g of ground sediment with a Bartington MS2 magnetic susceptibility meter (0.47/4.7 kHz). Particle-size distribution of the samples was analyzed using a Backman Coulter-LS laser analyzer. The chronological framework in the FJJ profile was established initially by pedo-stratigraphic correlation with the well-dated Holocene loess-soil profile at the Chendongcun site (CDC) in the middle Yellow River (Figs. 1, 4; Wang et al. 2012).

Five samples for OSL dating were taken from the profile at the FJJ site during the fieldwork. OSL samples were uncovered under subdued red light in the OSL laboratory of Shaanxi Normal University. The outer 2–3 cm were removed and the interior used for further processing, including pretreatment with 10 % HCl (to remove carbonates), 30 % H<sub>2</sub>O<sub>2</sub> (to remove organic material) and wet sieving to obtain the 125–225 μm grain fraction. The 125–225 μm grain fraction was etched by 40 % HF for 40 min to remove feldspar grains and then treated with 10 % HCl to remove acid-soluble fluoride precipitates. The purity of quartz grains was examined by detecting

**Fig. 3** **a** Horizontal palaeoflood SWD beds inserted in the slop clastic deposit at the FJJ site in the Shanxi-Shaanxi Gorge of the middle Yellow River river-bank. **b** Details of palaeoflood SWDs with a thin clay cap on top of a bed. **c** Modern flood SWD formed on the channel side during the 2012 flood along the Shanxi-Shaanxi Gorge of the middle Yellow River

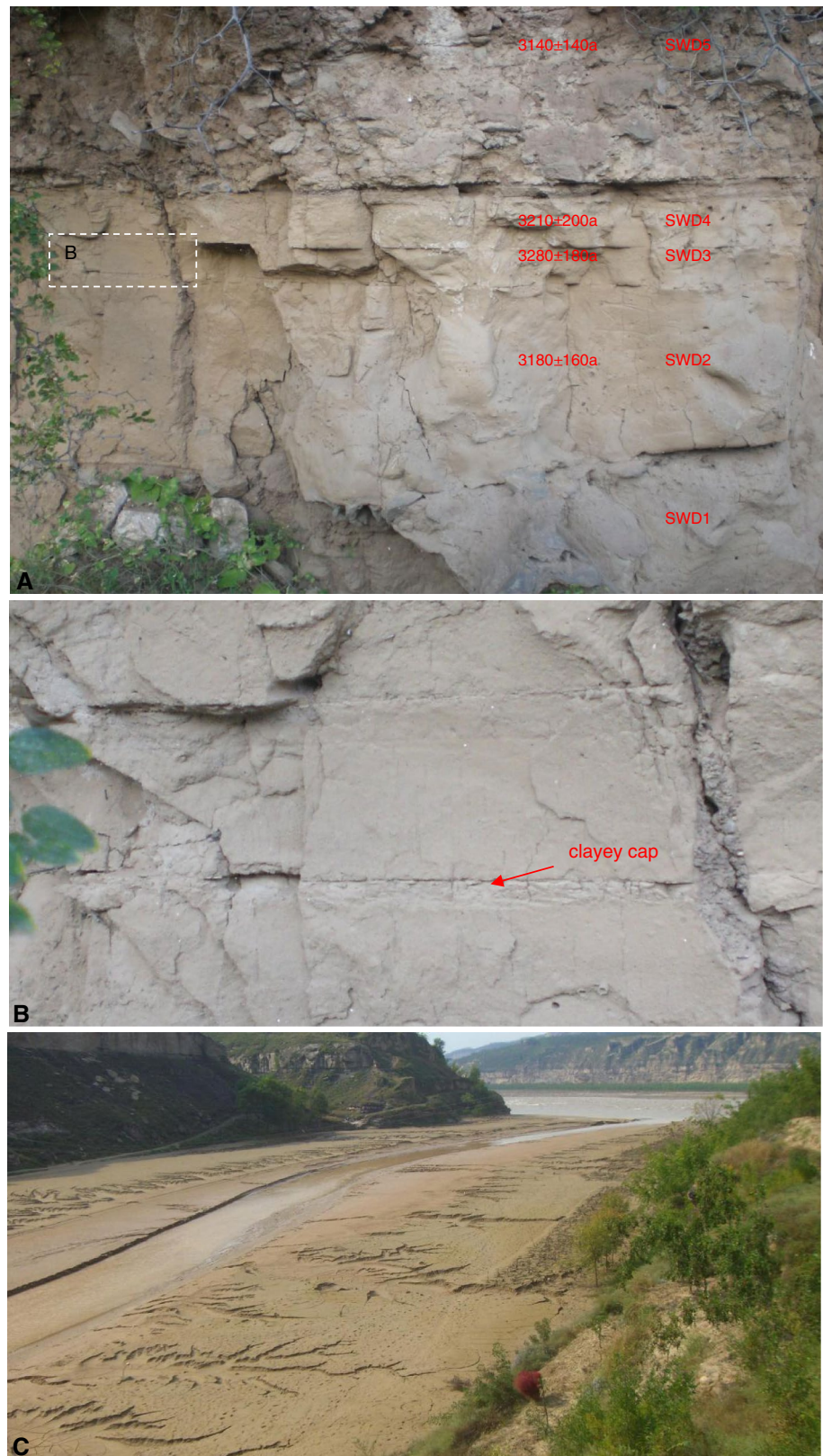
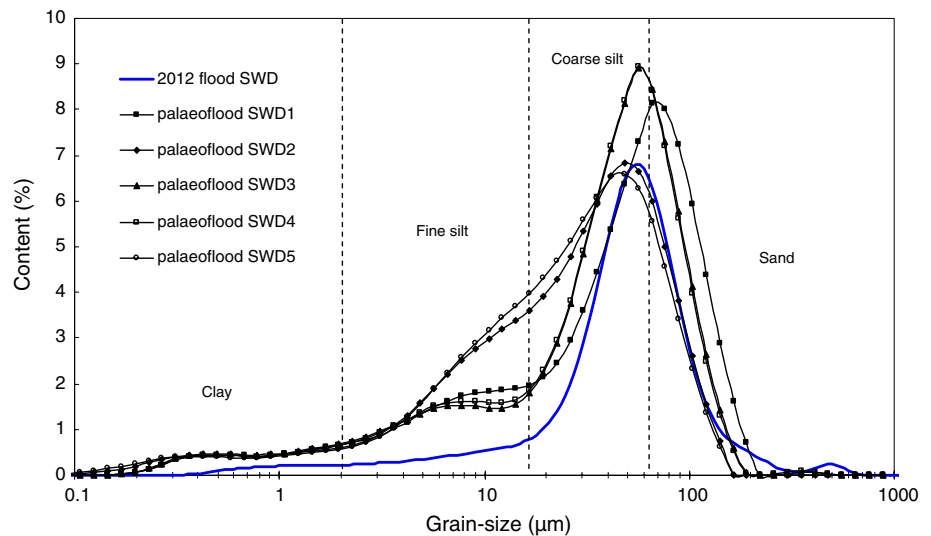


**Fig. 4** Particle-size distribution frequency of the palaeoflood SWDs in comparison with that of the 2012 flood SWD at the FJJ site in the Shanxi-Shaanxi Gorge of the middle Yellow River



the infrared-stimulated luminescence (IRSL) signal and the shape of the 110 °C TL peak (Mejdahly and Christiansen 1994). Quartz grains were then mounted on the center (2 mm in diameter) of aluminum aliquots (9.7 mm diameter) with silicone oil. The single-aliquot regenerative-dose (SAR) protocol (Murray and Wintle 2000; Banerjee et al. 2001) was used for paleodose determination.

All measurements were taken on a Risø-TL/OSL-DA20 dating system equipped with a combined blue ( $470 \pm 20$  nm,  $50$  mW/cm<sup>2</sup>) and infrared ( $870 \pm 40$  nm,  $150$  mW/cm<sup>2</sup>) LED unit, and a <sup>90</sup>Sr/<sup>90</sup>Y beta source for irradiation (Bøtter-Jensen and Duller 1992). The samples were preheated at 240 °C for 10 s before measurement. Optically stimulated luminescence dating was measured at 125 °C for 40 s. Luminescence emission was detected with a Thorn-EMI 9235QB photomultiplier tube and two 3-mm Hoya U-340 glass filters. For the calculation of the equivalent dose (De), all the signals were integrated over the first five channels of stimulation out of the 250 channels used for the whole OSL decay curve. A background was subtracted based on the last five channels. The software for SAR protocol developed especially for the Risø-TL/OSL system by Dr. G.A.T. Duller was used. The content of U, Th and K in the samples was determined with an inductively coupled plasma mass spectrometry (ICP-MS), which error was within 5 %. Cosmic dose rate is related to altitude, location and burial depth, which can be calculated by a certain transformation parameters (Prescott and Hutton 1994). Water content of the fresh samples was measured after drying at 105 °C for 12 h. Effective dose rate (Dy) was calculated from the elemental concentrations by using the revised dose-rate conversion factors (Adamiec and Aitken 1998). The computer program Age.exe (Grün 2003) was used for calculation of OSL dates.

## Results and discussions

### Identification of the palaeoflood events by SWDs

Palaeoflood SWD is a major evidence used for inference about hydrological parameters of the past flood events (Benito et al. 2004; Baker 2006). This fine-grained sediment is deposited at high flood stage from suspended load in overbank floodwater. It could be buried and preserved by various surface processes in the Holocene pedo-stratigraphy in the riverbanks. Field investigations along the Shanxi-Shaanxi Gorges of the Yellow River showed that the modern river channel is formed in bedrock. Slope clastic deposits were often seen at the base of the bedrock cliffs. Subangular gravel deposits from tributary rivers and gullies were always seen at the confluences. On the river banks along the mainstream in the Shanxi-Shaanxi Gorge of the middle Yellow River, the silt palaeoflood SWD beds were found interbedded in the Holocene loess-soil profiles and slope clastic sediments at many sites (Fig. 1b).

In the FJJ profile, which is ca 20 m above the normal river water level, a set of five palaeoflood slackwater deposit beds (SWDs) was identified by using the sedimentological criteria and by comparison with the modern flood SWD deposited on the channel sides in the 2012 flood. Very similar to the 2012 flood SWD along the Shanxi-Shaanxi Gorge of the middle Yellow River, the palaeoflood SWDs consist of well-sorted silt with pale orange color and parallel beddings (Fig. 3; Table 1). Each of the palaeoflood SWD beds is ca 15–50 cm in thickness and consists of compacted sterile silt with massive structure. It is clearly separated from the underlying and/or overlying bed by distinct stratigraphic breaks. A clayey cap of ca 0.5–1.0 cm in thickness formed on top of the SWD bed because of the sorted deposition in the palaeoflood slackwater (Fig. 3b).

**Table 1** Analytical results of the palaeoflood SWDs and 2012 flood SWD at the FJJ site in the Shanxi-Shaanxi Gorge of the middle Yellow River

Samples	Magnetic susceptibility ( $\times 10^{-8} \text{ m}^3/\text{kg}$ )	<2 ( $\mu\text{m}$ , %)	2–16 ( $\mu\text{m}$ , %)	16–63 ( $\mu\text{m}$ , %)	>63 ( $\mu\text{m}$ , %)	Md ( $\mu\text{m}$ )	Mz ( $\mu\text{m}$ )	Sk	Kg	QD
Palaeoflood SWD5	34.5	7.24	28.85	50.30	13.61	25.36	28.65	0.35	1.17	1.12
Palaeoflood SWD4	42.3	6.36	18.75	51.87	23.03	38.98	38.49	0.51	1.31	0.98
Palaeoflood SWD3	42.2	6.71	18.13	51.37	23.79	39.49	39.03	0.52	1.34	0.98
Palaeoflood SWD2	39.2	7.26	27.91	49.66	15.17	27.00	29.90	0.38	1.13	1.15
Palaeoflood SWD1	35.5	6.59	19.49	41.07	32.85	44.13	43.87	0.50	1.15	1.16
2012 flood SWD	33.7	2.88	8.73	49.60	38.79	54.01	56.86	0.31	1.79	0.58

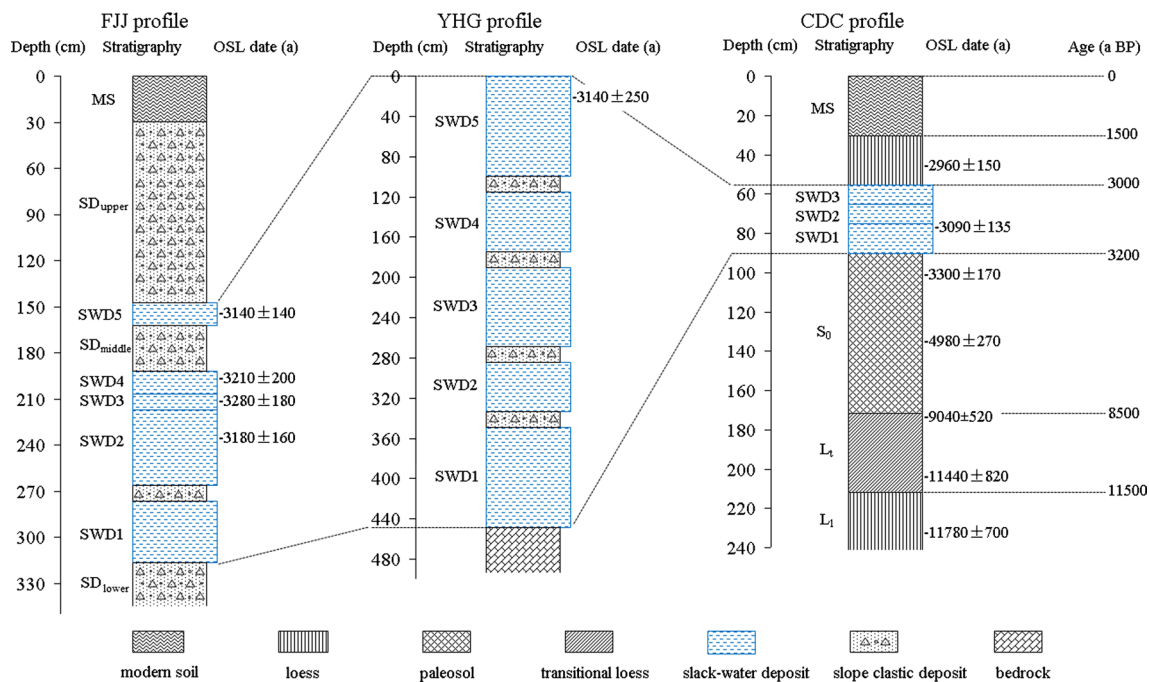


**Fig. 5** Stratigraphic subdivisions in the FJJ profile and its correlation with the YHG profile in the Shanxi-Shaanxi Gorge and the studied Holocene loess-soil profile at the Chendongcun site (CDC) in the

Weihe River valley, in the middle Yellow River (Huang et al. 2012c; Wang et al. 2012)

There are presence of slope wash between SWD1 and SWD2, between SWD4 and SWD5 (Figs. 3a, 5). These indicate that a single SWD bed resulted from one overbank flooding event.

Magnetic susceptibility is often used to manifest the intensity of weathering and pedogenic modification to accumulated dust and to identify palaeoflood SWD in loess-paleosol sequences. Magnetic susceptibility values in the palaeoflood SWD beds vary in the range of 34.5–42.3  $\times 10^{-8} \text{ m}^3/\text{kg}$ , much similar to that of the 2012 flood SWD (33.7  $\times 10^{-8} \text{ m}^3/\text{kg}$ ) (Table 1), which is lower than the general value of eolian loess (40–100  $\times 10^{-8} \text{ m}^3/\text{kg}$ ) and much lower than the general value of mid-Holocene Udic Luvisol (100–140  $\times 10^{-8} \text{ m}^3/\text{kg}$ ) in the Loess Plateau

(Huang et al. 2010). This verifies that the palaeoflood SWDs are relatively fresh without being affected by weathering and pedogenesis in situ. This means that they deposited in a very short time period and preserved immediately after flood recession (Ely and Baker 1985).

Particle-size distribution is a major sedimentary index used for differentiating palaeoflood SWD from sediments deposited by the other surface processes along the river valley. The particle-size distribution frequency in the palaeoflood SWDs at the FJJ site is shown in Fig. 4. The curves of the palaeoflood SWDs and the 2012 flood SWD overlap peak between 40 and 70  $\mu\text{m}$ , show a feature of well-sorted coarse silt. The particle-size distribution and the statistical indices such as median (Md), mean (Mz), skewness (Sk),

**Table 2** Summary of dosimetry, equivalent dose simulated with infrared light and OSL ages in the FJJ profiles in the Shanxi-Shaanxi Gorge of the middle Yellow River

Samples	Depth (m)	Number of aliquots	Number of calculated aliquots	Skewness	RSD (relative standard deviation) (%)	U (mg/kg)	Th (mg/kg)	K (%)	Water content (%)	Equivalent dose De (Gy)	Dose rate Dy (Gy/Ka)	OSL age (a)
Palaeoflood SWD5	1.575	40	8	0.83	68.87	3.07 ± 0.12	11.5 ± 0.32	1.69 ± 0.05	15.0	9.37 ± 0.38	3.18 ± 0.06	3,140 ± 140
Palaeoflood SWD4	1.975	50	7	1.25	85.64	3.08 ± 0.13	10.8 ± 0.35	1.75 ± 0.04	16.2	9.46 ± 0.56	2.80 ± 0.06	3,210 ± 200
Palaeoflood SWD3	2.125	50	10	2.38	84.77	3.51 ± 0.13	12.7 ± 0.38	1.75 ± 0.04	16.8	10.54 ± 0.53	2.83 ± 0.06	3,280 ± 180
Palaeoflood SWD2	2.275	48	12	0.45	56.92	3.24 ± 0.11	10.1 ± 0.30	1.76 ± 0.05	17.0	9.26 ± 0.43	2.92 ± 0.06	3,180 ± 160
Palaeoflood SWD1	2.875	31	10	0.13	19.21	2.62 ± 0.11	9.51 ± 0.29	1.63 ± 0.05	17.5	68.06 ± 0.12	2.62 ± 0.06	26,020 ± 550

kurtosis (Kg) and sorting (QD) are shown in Table 1, also show that the palaeoflood SWDs and the 2012 flood SWD have similar characteristics. Coarse silt (16–63  $\mu\text{m}$ ) is the main component of the palaeoflood SWDs and the 2012 flood SWD and minimum percentage of clay (<2  $\mu\text{m}$ ). This clearly indicates that the palaeoflood SWDs in the FJJ profile were deposited by overbank palaeoflood events on the Yellow River.

By an integration of the sedimentary features and analytical results, especially by a comparison to that of the 2012 flood SWD in the same reaches and that of the raised flood plain deposit, the palaeoflood events is represented by palaeoflood SWDs at the Fengjiaji site in the Shanxi-Shaanxi Gorge of the middle Yellow River.

#### Age of the palaeoflood events

#### *De determination and age calculation*

Equivalent dose was determined using the SAR protocol (Murray and Wintle 2000). An important factor influencing the distribution of the De values is the degree of natural bleaching of the OSL signal at the time of deposition (Pflanz et al. 2013). The sediments deposited by fluvial processes often have the problem or incomplete bleaching of grains (Kunz et al. 2013). OSL dating of fluvial sediments can be difficult because the De values may be overestimated due to the residual signals arising from partial bleaching of the sediments at the time of deposition. We also identified partial bleaching of the palaeoflood SWD at the time of deposition in the study profile. The Skewness of the De values were between 0.13 and 2.38, which indicated that luminescence signal of sediments are not zero before being buried (Table 2). Relative standard deviation (RSD) of the De values were between 19.21 and 85.64 %, which indicated that samples were insufficient bleaching (Table 2).

The minimum age model (MAM-3) was originally developed for fluvial deposits, where only a portion of the grains was assumed to be well bleached at the time of deposition (Galbraith et al. 1999; Feathers et al. 2006; Arnold et al. 2009). We used this model to calculate the proportion (*p* value) of well bleached aliquots in the FJJ profile, which resulted in the usage of 10, 12, 10, 7 and 8 aliquots for samples SWD1, SWD2, SWD3, SWD4 and SWD5, respectively, and the rejection of the other populations of partially bleached aliquots. The dosimetry and OSL dates from the sediment profile at the FJJ site are present in Table 2. Samples from palaeoflood SWD bedsets 2, 3, 4 and 5 were OSL dated to  $3,180 \pm 160$  a,  $3,280 \pm 180$  a,  $3,210 \pm 200$  a and  $3,140 \pm 140$  a, respectively. However, sample from palaeoflood SWD1 was OSL dated to  $26,020 \pm 550$  a, which was excessively large. The reason



is that a large number of debris weathered from mudstone and sandstone mixed with palaeoflood SWD1, while suspended sediment deposited at high flood water levels in the Yellow River. Sampling and processing cannot be separated, resulting in serious large De value in palaeoflood SWD1. Therefore, the OSL age value of palaeoflood SWD1 can be discarded, and close to palaeoflood SWD2 because of short distance between OSL samples of palaeoflood SWD1 and palaeoflood SWD2. These suggest that the palaeoflood events represented by SWD bedsets 1–5 occurred between 3200 and 3000 a BP.

#### *Climate nature of the palaeoflood events*

The 3,200–3,000 a BP floods were not unique events at Fengjiaji (FJJ) site, and at the Yongheguan (YHG) site and the Mafentan (MFT) site, extreme floods of same age were also reported on the Yellow River (Figs. 1, 5) (Huang et al. 2012c; Li et al. 2010). On the Weihe River, the Jinghe River and the Qishuihe River, which are tributaries in the middle reach of the Yellow River, extraordinary floods of the same age were documented by palaeohydrological investigations (Huang et al. 2011, 2012a, b). These show that the 3,200–3,000 a BP floods were widespread hydrological phenomena over the middle Yellow River basin. At many Holocene loess-soil profile on the Loess Plateau, the boundary between the mid-Holocene Luvisol ( $S_0$ ) and the recent loess ( $L_0$ ), which was dated to ca 3100 a BP, often indicates abrupt change of monsoonal climate from the mid-Holocene climatic optimum to the late Holocene dry conditions (Fig. 5) (Huang et al. 2003, 2004, 2009). The extraordinary floods documented in the Shanxi-Shaanxi Gorge of the middle Yellow River occurred just in the same episode of climatic aridity and pedogenic regression that were forced by monsoonal shift. It is therefore inferred that the monsoonal shift and the resultant climatic variability at about 3100 a BP are responsible for the occurrence of the intensive rainstorms and extraordinary floods in this semi-arid and subhumid region.

In early Chinese history, this time is just the demise of the Shang dynasty (3,550–3,000 a BP) with frequent droughts, drying-up of the Yellow River, intensified dust storms, harvest failures, great famine, plague and social upheavals. It was even read that “collapse of the Shang dynasty because of the drying-up of the Yellow River” in the well-known ancient literature (Huang et al. 2003). These facts show that both floods and droughts occurred over the middle to lower reaches of the Yellow River during the monsoonal climatic decline at ca 3,200–3,000 a BP.

Numerous paleoclimate archives of Holocene climatic change in different regions have defined the prominent 3200–2800 a BP event as an abrupt or rapid climatic event. For example, the  $\delta^{18}\text{O}$  time series of speleothem from

Dongge Cave in southern China (Wang et al. 2005), the  $\delta^{18}\text{O}$  signal at the Greenland ice cap (Johnsen et al. 1992) and the sodium ( $\text{Na}^+$ ) ion proxy in the GISP2 ice cores from the Greenland ice cap (Meeker and Mayewski 2002) have indentified the prominent event. The extreme floods documented on the Yellow River and its other tributaries, such as the Weihe River, the Jinghe River and the Qishuihe River, in this episode show that both droughts and floods occurred during this remarkable climatic decline because of high climatic variability.

#### Hydrologic reconstruction of the palaeofloods

The palaeoflood stage can be converted into flood discharge, which is the random variable used in the statistical analysis (Francés 2004). The reconstruction of palaeoflood stage depended on the elevation, the thickness and the attitude of palaeoflood SWD in the past. The palaeoflood minimum peak discharge could be calculated by the palaeoflood stage using the elevation of SWD top surface (Kochel and Baker 1982; Benito et al. 2003b). The palaeoflood discharge could be accurately calculated by the elevation of endpoint of palaeoflood SWD as the palaeoflood stage (Yang et al. 2000). The layer of palaeoflood SWD shows an endpoint with the trend of diminution in thickness up valley sometimes. This is an improvement over the former method, but the endpoints of palaeoflood SWD could not always be formed and preserved in steep wall and rock shelters in the bedrock canyon river channel, which is in favor of the hydrological recovery. The field survey of the relationship between the elevation and thickness of endpoints of 2012 flood SWD and the peak water level in the Shanxi-Shaanxi Gorge of the middle Yellow River showed that the elevations of endpoints were 0.7–1.2 m lower than the peak water level elevation, even the endpoints formed in broad valley or the tributary mouths. Using palaeoflood slackwater depth figured out using SWD thickness and bulk of suspended sediment load of the floodwater, therefore, the palaeoflood stage was determined, and then, the palaeoflood discharge was calculated. So the method is more accordance with actual circumstance than the form ones (Huang et al. 2012c; Li et al. 2010). Our field investigations at the Fengjiaji site (FJJ) showed that the endpoints of palaeoflood SWD could not be formed or preserved, where the river channel is narrow, deep and stable. Using the method of palaeoflood slackwater depth, the palaeoflood stage was calculated at the FJJ site (Table 3).

The accuracy of the discharge estimations depends on the cross-sectional stability through time (Benito and Thorndycraft 2005). In stable bedrock-confined channels, such as in the Shanxi-Shaanxi Gorge of the Yellow River, channel geometry at maximum stage is known or can be

**Table 3** Reconstructed peak discharges of the Holocene paleofloods and 2012 flood at the Fengjiaji section (FJJ) in the Shanxi-Shaanxi Gorge of the middle Yellow River

Paleoflood events	Paleoflood SWD thickness (m)	Paleoflood slackwater depth (m)	Paleoflood stage (m asl)	Total flood water depth (m)	River gradient	Roughness values	Cross-sectional area (m <sup>2</sup> )	Wetted perimeter (m)	Hydraulic radius (m)	Paleoflood peak discharge (m <sup>3</sup> /s)
SWD5	0.15	0.88	488.43	24.4	0.0012	0.035	6,789.21	377.99	17.96	46,090
SWD4	0.15	0.88	487.98	24.0	0.0012	0.035	6,626.36	373.28	17.75	44,630
SWD3	0.1	0.59	487.59	23.6	0.0012	0.035	6,485.99	370.38	17.51	43,290
SWD2	0.5	2.94	489.44	25.4	0.0012	0.035	7,160.73	384.10	18.64	49,830
SWD1	0.4	2.35	488.35	24.4	0.0012	0.035	6,760.11	374.77	18.04	46,020
2012 flood	–	–	473.5	9.5	0.0012	0.035	2,015.07	289.17	6.97	7,280

approximated because no major changes can be assumed to have occurred in the Holocene. Cross-sectional O–O' was chosen for palaeoflood hydrological reconstruction at the FJJ site (Fig. 2). The river channel geometric and hydraulic parameters, i.e.,  $S$  were measured at the FJJ site using an electronic distance measurer and GPS in association with the 1:10,000 scale map. The roughness values (Manning's  $n$  value) of the channel were assigned by referring to the hydrological calculation norms for hydraulic engineering in China (Table 3).

A number of hydraulic formulae and models are used to calculate palaeoflood discharge from the known palaeoflood stage in the bedrock channel. The FJJ site is relatively uniform reaches. When a great flood occurs, the flood overflows the whole channel. There is a little change in channel width within 1 km from upstream to downstream at the FJJ site, basically between 350 and 370 m (Fig. 2a, b). Running HEC RAS version 4.1.0 showed that channel flow velocity was between 5.64 and 6.85 m/s, and Froude Number was between 0.42 and 0.50 at the FJJ site. This indicates that the study reach is subcritical flow, i.e., bed slope, energy slope and water surface slope are all approximately equal. In this study, the slope–area method of streamflow measurement was adopted and the formulae is as follows (Manning 1889)

$$Q = 1/n (AR^{2/3}S^{1/2})$$

in which  $Q$  is flood peak discharge (m<sup>3</sup>/s),  $n$  is roughness values (Manning's  $n$  value),  $A$  is a cross-sectional area (m<sup>2</sup>),  $R$  is hydraulic radius (m), and  $S$  is water surface gradient. Using the method of palaeoflood slackwater depth for the palaeoflood stage, along with the river channel geometric and hydraulic parameters, the palaeoflood peak discharges were estimated to range from 43,290 to 49,830 m<sup>3</sup>/s with the slope–area method (Table 3). This is very close to the discharges reconstructed by palaeoflood SWD at the YHG site and the MFT site in the Shanxi-Shaanxi Gorge in the middle Yellow River (Fig. 1b) (Huang et al. 2012c; Li et al. 2010). These reconstructed palaeoflood peak discharges are 2.0–2.5 times the largest gauged flood (21,000 m<sup>3</sup>/s) that has ever occurred since 1934 at the Longmen gauge station on the Yellow River.

In order to check the reliability of the slope–area method of streamflow measurement for palaeoflood discharge estimation at the FJJ site, the peak discharge of the 2012 flood was also reconstructed using the same method. The peak stage of the 2012 flood in the Shanxi-Shaanxi Gorge of the middle Yellow River was indicated by the flood mark and botanical evidence. The reconstructed peak discharge of 7,280 m<sup>3</sup>/s was very close to the gauged discharge of 7,620 m<sup>3</sup>/s in 2012 at the Longmen gauge station. This showed that the palaeoflood discharge estimation was very reliable.

## Conclusions

Palaeoflood SWDs were identified by sedimentary criteria that have been used in palaeohydrology at several sites along the Shanxi-Shaanxi Gorge of the middle Yellow River. These bedded silt deposits were sourced from a suspended sediment load in floodwater flow. Analytical results show that magnetic susceptibility and particle-size distribution in the palaeoflood SWD beds are similar to that of the SWDs formed during the 2012 floods in the same reach. Using the method of palaeoflood slackwater depth for the palaeoflood stage, the palaeoflood peak discharges were estimated to range from 43,290 to 49,830 m<sup>3</sup>/s with the slope–area method. It is similar to the flood magnitude as that reconstructed at the YHG site and the MFT site in the upstream and downstream, respectively. These reconstructed palaeoflood peak discharges are 2.0–2.5 times the largest gauged flood (21,000 m<sup>3</sup>/s) on the Yellow River. These extraordinary flood events were dated to 3,200–3,000 a by using the OSL method and checked by pedostratigraphic correlations with the other dated loess-soil profiles in the catchment. On the mainstream and tributaries of the middle Yellow River, extraordinary flood events of the same age were also documented by palaeohydrological investigations. During this episode, monsoonal climate shifted from the mid-Holocene Climatic Optimum to the late Holocene dry conditions. The collapse of the Shang dynasty was coherent with this climatic decline and was attributed to the droughts occurred over the middle to lower reaches of the Yellow River at the same time. The extraordinary floods documented in this episode also show that both the severe droughts and the extreme floods are parts of the climatic variations during global climatic change.

**Acknowledgments** This study was supported by Grants from the Natural Science Foundation of China (Nos. 41471071, 41030637), the Ph.D. Programs Foundation of the Chinese Ministry of Education (No. 20110202130002).

## References

- Adamiec G, Aitken MJ (1998) Dose-rate conversion factors: update. *Anc TL* 16:37–50
- Arnold LJ, Roberts RG, Galbraith RF, DeLong SB (2009) A revised burial dose estimation procedure for optical dating of young and modern-age sediments. *Quat Geochronol* 4:306–325
- Baker VR (1987) Palaeoflood hydrology and extraordinary flood events. *J Hydrol* 96:79–99
- Baker VR (2006) Palaeoflood hydrology in a global context. *Catena* 66(1/2):161–168
- Baker VR (2008) Palaeoflood hydrology: origin, progress, prospects. *Geomorphology* 101:1–13
- Baker VR, Kochel RC (1988) Flood sedimentation in bedrock fluvial systems. In: Baker VR, Kochel RC, Patton PC (eds) *Flood geomorphology*. Wiley, New York, pp 123–137
- Banerjee D, Murray AS, Bøtter-Jensen L, Lang A (2001) Equivalent dose estimation using a single aliquot of polymineral fine grains. *Radiat Meas* 33:73–94
- Benito G, Thorndycraft VR (2005) Palaeoflood hydrology and its role in applied hydrological sciences. *J Hydrol* 313:3–15
- Benito G, Sopena A, Sánchez-Moya Y (2003a) Sedimentology of high-stage flood deposits of the Tagus River, Central Spain. *Sediment Geol* 157:107–132
- Benito G, Sopena A, Sánchez-Moya Y, Machado MJ, Pérez-González A (2003b) Palaeoflood record of the Tagus River (central Spain) during the late Pleistocene and Holocene. *Quat Sci Rev* 22:1737–1756
- Benito G, Lang M, Barriendos M, Llasat MC, Francés F, Ouarda T, Thorndycraft VR, Enzel Y, Bardossy A, Coeur D, Bobée B (2004) Use of systematic palaeoflood and historical data for the improvement of flood risk estimation: review of scientific methods. *Nat Hazards* 31:623–643
- Bøtter-Jensen L, Duller GAT (1992) A new system for measuring optically stimulated luminescence from quartz samples. *Nucl Tracks Radiat Meas* 20:549–553
- Ely LL, Baker VR (1985) Reconstructing palaeofloods hydrology with slackwater deposits: Verde River, Arizona. *Phys Geogr* 6:103–126
- Feathers JK, Rhodes EJ, Huot S, Mcavoy JM (2006) Luminescence dating of sand deposits related to late Pleistocene human occupation at the Cactus Hill Site, Virginia, USA. *Quat Geochronol* 1:167–187
- Francés F (2004) Flood frequency analysis using systematic and non-systematic information. In: Benito G, Thorndycraft VR (eds) *Systematic palaeoflood and historical data for the improvement of flood risk estimation*. CSIC, Madrid, pp 55–70
- Galbraith RF, Roberts RG, Laslett GM, Yoshida H, Olley JM (1999) Optical dating of single and multiple grains of quartz from Jinmium rock shelter, northern Australia: part I, experimental design and statistical models. *Archaeometry* 41:339–364
- Grün R (2003) The age exe computer program for the calculation of luminescence dates. RSES, Canberra
- Huang CC, Zhao SC, Pang JL, Zhou QY, Chen SE, Li PH (2003) Climatic aridity and the relocations of the Zhou Culture in the Southern Loess Plateau of China. *Clim Change* 61(3):361–378
- Huang CC, Pang JL, Zhou QY, Chen SE (2004) Holocene pedogenic change and the emergence and decline of rain-fed cereal agriculture on the Chinese Loess Plateau. *Quat Sci Rev* 23:2529–2539
- Huang CC, Pang JL, Zha XC, Su HX (2007) Impact of monsoonal climatic change on Holocene overbank flooding along the Sushui River within the middle reaches of the Yellow River, China. *Quat Sci Rev* 26:2247–2264
- Huang CC, Pang JL, Su HX, Mao LJ, Wang LJ (2009) The Ustic Isohumisol (Chernozem) distributed over the Chinese Loess Plateau: modern soil or palaeosol? *Geoderma* 150:344–358
- Huang CC, Pang JL, Zha XC, Zhou YL, Su HX, Li YQ (2010) Extraordinary floods of 4100–4000 a BP recorded at the late Neolithic ruins in the Jinghe River gorges, middle reach of the Yellow River, China. *Palaeogeogr Palaeoclimatol Palaeoecol* 289:1–9
- Huang CC, Pang JL, Zha XC, Su HX, Jia YF (2011) Extraordinary floods related to the climatic event at 4200 a BP on the Qishuihe River, middle reaches of the Yellow River, China. *Quat Sci Rev* 30:460–468
- Huang CC, Pang JL, Zha XC, Zhou YL, Su HX, Wan HL, Ge BW (2012a) Sedimentary records of the extraordinary floods at the ending of the mid-Holocene climatic optimum along the upper Weihe River China. *Holocene* 22(6):675–686
- Huang CC, Pang JL, Zha XC, Zhou YL, Su HX, Zhang YZ, Wang HS, Gu HL (2012b) Holocene palaeoflood events recorded by slackwater deposits along the lower Jinghe River valley, middle Yellow River basin, China. *J Quat Sci* 27(5):485–493

- Huang CC, Li XG, Pang JL, Zha XC, Zhou YL (2012c) Palaeoflood sedimentological and hydrological studies on the Yongheguan reach in the middle Yellow River. *Acta Geogr Sin* 67(11):1493–1504 (in Chinese with English abstract)
- Huang CC, Pang JL, Zha XC, Zhou YL, Yin SY, Su HX, Zhou L, Yang JC (2013) Extraordinary hydro-climatic events during the period AD 200–300 recorded by slackwater deposits in the upper Hanjiang River valley, China. *Palaeogeogr Palaeoclimatol Palaeoecol* 374:274–283
- Johnsen S, Clausen H, Dansgaard W, Fuhrer K, Gundestrup N, Hammer C, Iversen P, Jouzel J, Stauffer B, Steffensen J (1992) Irregular glacial interstadials recorded in a new Greenland ice core. *Nature* 359:311–313
- Jones AP, Shimazu H, Oguchi T, Okuno M, Tokutake M (2001) Late Holocene slackwater deposits on the Nakagawa River, Tochigi prefecture, Japan. *Geomorphology* 39:39–51
- Kale VS, Singhvi AK, Mishra PK, Banerjee D (2000) Sedimentary records and luminescence chronology of late Holocene palaeofloods in the Luni River, Thar Desert, northwest India. *Catena* 40:337–358
- Knox JC (2000) Sensitivity of modern and Holocene floods to climatic change. *Quat Sci Rev* 19:439–457
- Kochel RC, Baker VR (1982) Palaeoflood hydrology. *Science* 215:353–361
- Kunz A, Pflanz D, Weniger T, Urban B, Krüger F, Chen YG (2013) Optically stimulated luminescence dating of young fluvial deposits of the Middle Elbe River Flood Plains using different age models. *Geochronometria* 41:36–56
- Li XG, Huang CC, Pang JL, Zha XC, Hao GJ, Ge BW (2010) Hydrological Studies of the Holocene palaeoflood in the Hukou Reach of the Yellow River. *Acta Geogr Sin* 62(3):291–300 (in Chinese with English abstract)
- Manning R (1889) On the flow of water in open channels and pipes. *Trans Inst Civ Eng Irel* 20:161–207
- Meeker LD, Mayewski PA (2002) A 1400-year high-resolution record of atmospheric circulation over the North Atlantic and Asia. *Holocene* 12:257–266
- Mejdahly V, Christiansen HH (1994) Procedures used for luminescence dating of sediments. *Quat Sci Rev* 13:406
- Murray AS, Wintle AG (2000) Luminescence dating of quartz using an improved single-aliquot regenerative-dose protocol. *Radiat Meas* 32:57–73
- Peng GH, Xia J, Ma XF, Ma JQ (2011) Analysis on drought frequency distribution and digital characteristics of number of turns of the Yellow River Basin. *Yellow River* 06:3–5 (in Chinese with English abstract)
- Pflanz D, Gaedicke C, Freitag R, Krbetschek M, Tsukanov N, Baranov B (2013) Neotectonics and recent uplift at Kamchatka and Aleutian arc junction, Kamchatka Cape area, NE Russia. *Int J Earth Sci* 102:903–916
- Prescott JR, Hutton JT (1994) Cosmic ray contributions to dose rates for luminescence and ESR dating: large depths and long-term time variations. *Radiat Meas* 23(2–3):497–500
- Sheffer NA, Rico M, Enzel Y, Benito G, Grodek T (2008) The palaeoflood record of the Gardon River, France: a comparison with the extreme 2002 flood event. *Geomorphology* 98:71–83
- Wang YJ, Cheng H, Edwards RL, He YQ, Kong XG, An ZS, Wu JY, Kelly MG, Dykoski CA, Li XD (2005) The Holocene Asian monsoon: links to solar changes and North Atlantic climate. *Science* 308:854–857
- Wang HS, Huang CC, Zhou YL, Pang JL, Zha XC, Gu HL (2012) OSL dating of the Holocene Palaeoflood events: a case study of the Lintong Segment in the Lower Weihe River Valley. *Acta Geosci Sin* 33(2):227–235 (in Chinese with English abstract)
- Xu JH, Li XY, Chen JJ (2009) Effects of engineering on storm rains and floods in the Middle Reaches of the Yellow River—the Hekou to Longmen part. *Yellow River Conservancy Press, Zhengzhou*, pp 1–340 (in Chinese)
- Yang DY, Yu G, Xie YB, Zhan DJ, Li ZJ (2000) Sedimentary records of large Holocene floods from the middle reaches of the Yellow River, China. *Geomorphology* 33:73–88
- Yao P, Huang CC, Pang JL, Zha XC, Li XG (2008) Palaeoflood hydrological studies in the middle reaches of the Beiluohe River. *Acta Geogr Sin* 63:1198–1206 (in Chinese with English abstract)
- Yi YJ, Shi FC (1997) Reviews of flood investigations in the Yellow River. In: Shi FC, Yi YJ, Gao ZD (eds) *Storm rains and floods in the Yellow River*. Yellow River Hy-draulics Press, Zhengzhou, pp 193–216 (in Chinese)
- Zhang XH, Li GX, Zhang XF (1999) Changes of flood characteristics in the Middle Yellow River. *Yellow River* 08:13–14 (in Chinese)
- Zhang YZ, Huang CC, Pang JL, Zha XC, Zhou YL, Gu HL (2013) Holocene paleofloods related to climatic events in the upper reaches of the Hanjiang River valley, middle Yangtze River basin, China. *Geomorphology* 195:1–12